

BI-TP 99/47  
ER/40685/941  
LU-ITP 1999/023  
PSI-PR-99-34  
UR-1594  
hep-ph/9912447

## W-pair production at future $e^+e^-$ colliders: precise predictions from RACOONWW

A. DENNER<sup>1</sup>, S. DITTMAIER<sup>2</sup>, M. ROTH<sup>3</sup> AND D. WACKEROTH<sup>4</sup>

<sup>1</sup> *Paul Scherrer Institut  
CH-5232 Villigen PSI, Switzerland*

<sup>2</sup> *Theoretische Physik, Universität Bielefeld  
D-33615 Bielefeld, Germany*

<sup>3</sup> *Institut für Theoretische Physik, Universität Leipzig  
D-04109 Leipzig, Germany*

<sup>4</sup> *Department of Physics and Astronomy, University of Rochester  
Rochester, NY 14627-0171, USA*

### Abstract:

We present numerical results for total cross sections and various distributions for  $e^+e^- \rightarrow WW \rightarrow 4f(+\gamma)$  at a future 500 GeV linear collider, obtained from the Monte Carlo generator RACOONWW. This generator is the first one that includes  $\mathcal{O}(\alpha)$  electroweak radiative corrections in the double-pole approximation completely. Owing to their large size the corrections are of great phenomenological importance.

One of the most important class of processes to be investigated at future  $e^+e^-$  linear colliders are the four-fermion production processes, which involve in particular W-pair production,  $e^+e^- \rightarrow WW \rightarrow 4f$ . In order to match the experimental accuracy for this process of 1% or better, theoretical predictions for the corresponding cross sections of  $e^+e^- \rightarrow 4f$  with a precision at the level of some 0.1% are needed. This requires to include the complete set of lowest-order diagrams for  $e^+e^- \rightarrow 4f$  and the  $\mathcal{O}(\alpha)$  corrections to the W-pair production channels  $e^+e^- \rightarrow WW \rightarrow 4f$ . In addition, the leading higher-order corrections should be taken into account.

In all regions of phase space where W-pair production dominates the cross section for  $e^+e^- \rightarrow 4f$ , an expansion of the matrix element about the poles of the resonant W propagators provides a reasonable approximation for the radiative corrections. Neglecting corrections to the non-doubly-resonant contributions leads to uncertainties of the order  $\alpha/\pi \times \Gamma_W/M_W \times \log(\dots) \sim 0.1\%$  with respect to the leading lowest-order contributions, where the logarithm indicates possible logarithmic enhancements. This so-called double-pole approximation (DPA) provides a gauge-invariant answer and allows us to use the existing results for on-shell W-pair production [ 1, 2] and W-boson decay [ 3, 4], as far as the virtual corrections are concerned.

The DPA for  $\mathcal{O}(\alpha)$  corrections to pair production of unstable particles has already been proposed in Ref. [ 5]. Recently different variants of the DPA have been used in the literature [ 6, 7, 8, 9, 10]. A Monte Carlo generator including the corrections to the W-pair production subprocess and the leading-logarithmic corrections to the W-boson decays has been constructed in Refs. [ 7, 8], but non-factorizable corrections and W-spin correlations have been neglected there. With this generator also results for the centre-of-mass (CM) energy  $\sqrt{s} = 500$  GeV have been produced. A different, but also approximate, implementation [ 9] of the DPA has been compared at energies  $\sqrt{s} \gtrsim 500$  GeV with a high-energy approximation [ 11] for  $e^+e^- \rightarrow WW \rightarrow 4f$ . The first complete calculation of the  $\mathcal{O}(\alpha)$  corrections for off-shell W-pair production, including a numerical study of leptonic final states for LEP2 energies, was presented in Ref. [ 6] using a semi-analytical approach, which is, however, only applicable to ideal theoretical situations.

Recently the first Monte-Carlo generator that incorporates the complete  $\mathcal{O}(\alpha)$  corrections for off-shell W-pair production in DPA has been constructed. This generator, called RACOONWW [ 10, 12], includes the complete lowest-order matrix elements for  $e^+e^- \rightarrow 4f$  for any four-fermion final state. For the virtual corrections a DPA is used without any additional approximations. In particular, the exact four-fermion phase space is used throughout. The virtual corrections consist of factorizable and non-factorizable contributions. The former are the ones that are associated to either W-pair production or W-boson decay; the results of Refs. [ 1, 3] are used in this part. The latter comprise all corrections in which the subprocesses production and decays do not proceed independently. Up to some simple supplements, the virtual non-factorizable corrections can be read off from the literature [ 13, 14]; we made use of the results of Ref. [ 14] and included the exact off-shell Coulomb singularity [ 15]. The real bremsstrahlung corrections are based on the full matrix-element calculation for  $e^+e^- \rightarrow 4f\gamma$  described in Ref. [ 16]. More precisely, the minimal gauge-invariant subset including all doubly-resonant contributions of the processes  $e^+e^- \rightarrow WW \rightarrow 4f\gamma$ , i.e. the photon radiation from the CC11 subset, are included. By using the exact matrix elements for the real radiation, we avoid prob-

lems in defining a DPA for semi-soft photons ( $E_\gamma \sim \Gamma_W$ ) and, moreover, can include the leading logarithmic corrections to non-doubly-resonant diagrams (background diagrams) exactly. The real corrections and the virtual corrections are matched in such a way that all infrared singularities cancel exactly. The initial-state collinear singularities are regularized by retaining a finite electron mass and factorized into lowest-order matrix element and splitting functions. The collinear singularities connected to final-state radiation are treated inclusively, i.e. photons within collinear cones around the final-state fermions are integrated over, so that no logarithmic final-state fermion mass dependence survives. All contributions have been implemented in two programs, one of which uses the subtraction method described in Ref. [17], the other one uses phase-space slicing. All parts of the calculations have been performed in two independent ways. A detailed description of the calculation and the Monte Carlo generator RACOONWW will be published elsewhere [12]. Results for the LEP2-energy region have already been given in Ref. [10]. Here we concentrate on results for  $\sqrt{s} = 500$  GeV, which is relevant for a future linear collider.

For the numerical evaluation we used the same input as in Ref. [10], i.e. the fixed-width scheme and the following parameters:

$$\begin{aligned}
G_\mu &= 1.16637 \times 10^{-5} \text{ GeV}^{-2}, & \alpha &= 1/137.0359895, \\
M_W &= 80.35 \text{ GeV}, & \Gamma_W &= 2.08699 \dots \text{ GeV}, \\
M_Z &= 91.1867 \text{ GeV}, & \Gamma_Z &= 2.49471 \text{ GeV}, \\
m_t &= 174.17 \text{ GeV}, & M_H &= 150 \text{ GeV}, \\
m_e &= 510.99907 \text{ keV}. & &
\end{aligned} \tag{1}$$

The reliability of the fixed-width scheme at high energies has been demonstrated in Ref. [18]. The weak mixing angle is fixed by  $c_w = M_W/M_Z$ ,  $s_w^2 = 1 - c_w^2$ . The parameters in (1) are over-complete but self-consistent. Instead of  $\alpha$  we use  $G_\mu$  to parameterize the lowest-order matrix element, i.e. we use the effective coupling

$$\alpha_{G_\mu} = \frac{\sqrt{2}G_\mu M_W^2 s_w^2}{\pi} \tag{2}$$

in the lowest-order matrix element. This parameterization has the advantage that all higher-order contributions associated with the running of the electromagnetic coupling and the leading universal two-loop  $m_t$ -dependent corrections to the dominant contributions are correctly taken into account. In the relative  $\mathcal{O}(\alpha)$  corrections, on the other hand, we use  $\alpha$ , since in the real corrections the scale of the real photon is zero. The W-boson width given above is calculated including the electroweak and QCD one-loop corrections with  $\alpha_s = 0.119$ . We do not include QCD corrections to the process  $e^+e^- \rightarrow WW \rightarrow 4f$ , and initial-state radiation is only taken into account in  $\mathcal{O}(\alpha)$ .

In Table 1 we present numbers for total cross sections without any cuts based on 20 million events. In particular, we give the CC03 cross sections, i.e. the cross sections resulting from the signal diagrams only (defined in the 't Hooft–Feynman gauge). We also give numbers resulting from the complete set of diagrams for those final states where this is possible without cuts, i.e. the CC11 class of processes. In the considered cases, the effects of the background diagrams are below 0.6%. Note that we treat the external fermions as

final state	CC03 Born	full Born	CC03 corrected	full corrected
$\nu_\mu\mu^+\tau^-\bar{\nu}_\tau$	87.12(4)	86.66(3)	90.27(4)	89.81(4)
	87.11(4)	86.65(3)	90.19(5)	89.73(5)
$\nu_\mu\mu^+d\bar{u}$	261.4(1)	260.0(1)	270.6(1)	269.3(1)
	261.3(1)	260.0(1)	270.3(2)	269.0(2)
$u\bar{d}s\bar{c}$	784.1(3)	780.3(3)	811.3(4)	807.5(4)
	784.0(3)	780.4(3)	810.9(4)	807.2(4)
total	7057(2)		7305(2)	
	7056(2)		7299(3)	

Table 1: Total cross sections in fb for  $e^+e^- \rightarrow WW \rightarrow 4f$  without cuts for various final states at  $\sqrt{s} = 500$  GeV

massless. Therefore, the cross sections for processes not in CC11 class become singular if no cuts are imposed for final-state electrons collinear to the beams and for virtual photons splitting into  $f\bar{f}$  pairs with small invariant masses. The shown corrections are typically 3.5% at  $\sqrt{s} = 500$  GeV. The numbers in parentheses are estimates of the Monte Carlo integration errors. The numbers for the total W-pair (CC03) production cross section in the last two rows of the tables directly result from the other rows by multiplying these with the number of equivalent channels and adding them up. The numbers in the upper lines are from the subtraction-method branch of RACOONWW, the number in the lower lines from the phase-space slicing branch. The agreement between these numbers serves as a stringent consistency check of our generator.

Note that the total CC03 cross section of Table 1 is different from the full cross section for four-fermion production, as non-doubly-resonant (background) diagrams significantly contribute to the total cross section for high energies. The most important class of background diagrams are the ones for single-W production, which is dominant if electrons or positrons are scattered in the very forward directions (see e.g. Ref. [19] and references therein). The DPA approach is, of course, restricted to situations where the doubly-resonant diagrams dominate the cross section. Therefore, before confronting the  $\mathcal{O}(\alpha)$ -corrected prediction of RACOONWW with empirical data one has either to specify cuts that suppress background diagrams or to extract the W-pair signal from the full four-fermion signature.

Next, we study observables that involve phase-space and photon-recombination cuts. Because of our treatment of mass singularities (see Ref. [12] for details) it is necessary to combine photons that are collinear to the incoming or outgoing fermions appropriately with these fermions in order to obtain well-defined finite distributions. To this end we introduce the following recombination and cut procedure which proceeds in three steps:

1. All photons within a cone of 5 degrees around the beams are treated as invisible, i.e. their momenta are disregarded when calculating angles, energies, and invariant masses.

2. Next, the invariant masses of the photon with each of the charged final-state fermions are calculated. If the smallest one is smaller than  $M_{\text{rec}}$ , the photon is combined with the corresponding fermion, i.e. the momenta of the photon and the fermion are added and associated with the momentum of the fermion, and the photon is discarded.
3. Finally, all events are discarded in which one of the final-state fermions is within a cone of 10 degrees around the beams. No other cuts are applied.

We consider the cases of a tight recombination cut  $M_{\text{rec}} = 5 \text{ GeV}$ , of a loose recombination cut  $M_{\text{rec}} = 25 \text{ GeV}$ , and the case of full photon recombination,  $M_{\text{rec}} = 500 \text{ GeV}$ . In the following observables, the momenta of the W bosons are always defined by the sum of the momenta of the two corresponding decay fermions after the eventual recombination with the photon.

We now discuss various distributions for the  $\nu_\mu\mu^+\text{d}\bar{u}$  final state. These results have been obtained from 50 million events. In the following figures we always show on the left-hand side the absolute distributions in lowest order and including the corrections for the recombination cut  $M_{\text{rec}} = 5 \text{ GeV}$ , and on the right-hand side the corresponding relative corrections for the three recombination cuts  $M_{\text{rec}} = 5 \text{ GeV}$ ,  $M_{\text{rec}} = 25 \text{ GeV}$ , and  $M_{\text{rec}} = 500 \text{ GeV}$ .

In Figure 1 we present the distribution of events in the angle between the  $W^+$  and the incoming  $e^+$ . The corrections lead to a drastic increase of the cross section in the backward direction. This effect is due to hard-photon emission from the initial state, which boosts the CM-system of the W bosons and causes a migration of events from regions with large cross section in the CM system to regions with small cross section in the laboratory system. The relative corrections are very large there, because the lowest-order cross section is very small. Owing to the small cross section, this region of phase space is rather unimportant. Similar but less dramatic boost effects are also visible in the following distributions. The production-angle distribution depends on the recombination scheme only weakly, as expected. An increase of the recombination cut leads to a redistribution of events from the backward to the forward direction. Since there is more phase space for hard photons for higher scattering energies, the effects of a full recombination are more pronounced at  $\sqrt{s} = 500 \text{ GeV}$  than at LEP2 energies, discussed in Ref. [10]. This feature can also be observed in the following distributions.

The distribution of events in the angle between the  $W^+$  and the outgoing  $\mu^+$  is presented in Figure 2. In this case we find a noticeable dependence on the recombination mass  $M_{\text{rec}}$  for large decay angles, where the cross section is, however, very small. This originates from the fact that the recombination of a fermion with a photon parallel to this fermion decreases the angle between the fermion and the W boson from which the fermion results.

The distribution of events in the energy  $E_\mu$  of the outgoing  $\mu^+$  is depicted in Figure 3. In the on-shell approximation it would be restricted between  $6.6 \text{ GeV} < E_\mu < 243.4 \text{ GeV}$ . Again the radiative corrections tend to smooth the distribution. The recombination of a photon with the muon increases the muon energy. Consequently, an increase of the recombination mass  $M_{\text{rec}}$  shifts the distribution to larger muon energies, as can be seen in the relative corrections.

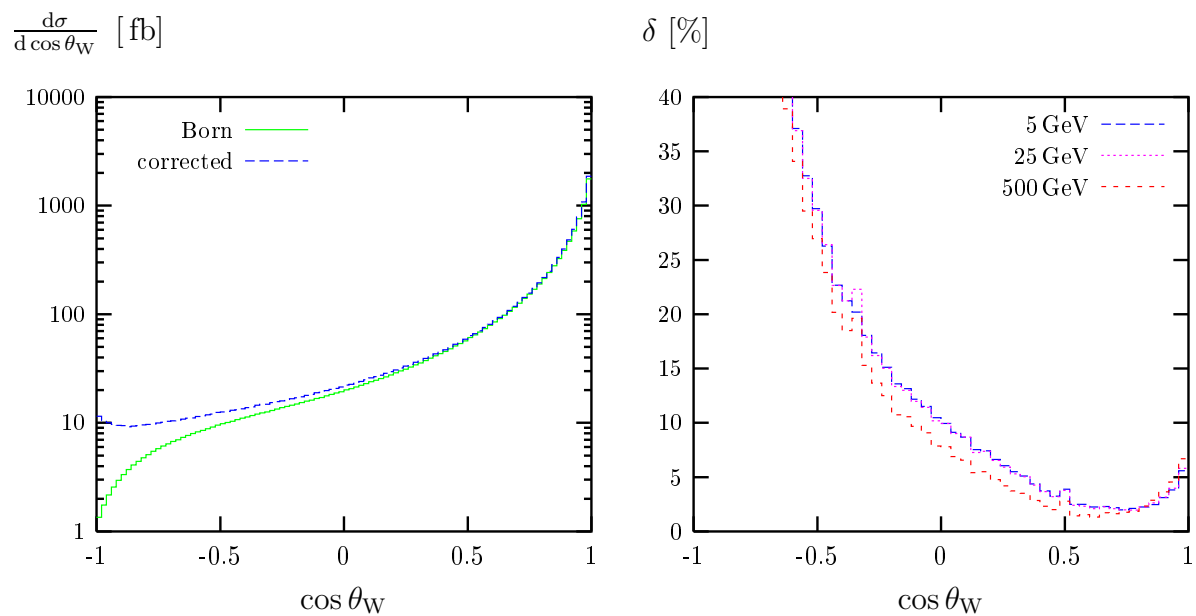


Figure 1: Production-angle distribution for  $e^+e^- \rightarrow \nu_\mu\mu^+d\bar{u}$  and  $\sqrt{s} = 500$  GeV

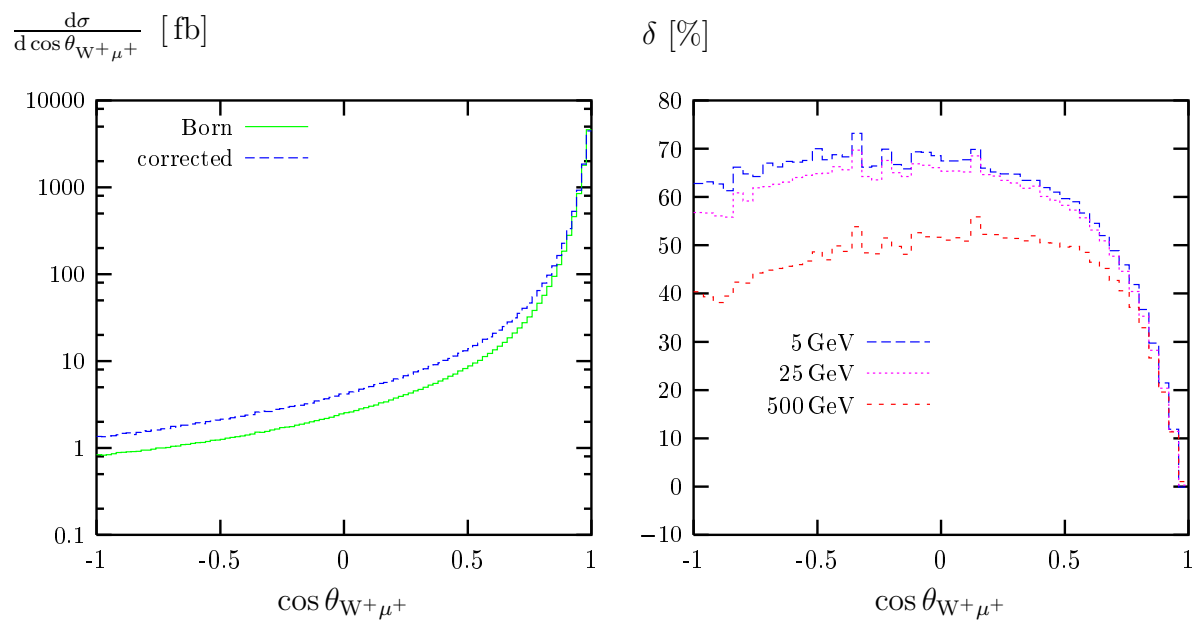


Figure 2: Decay-angle distribution for  $e^+e^- \rightarrow \nu_\mu\mu^+d\bar{u}$  and  $\sqrt{s} = 500$  GeV

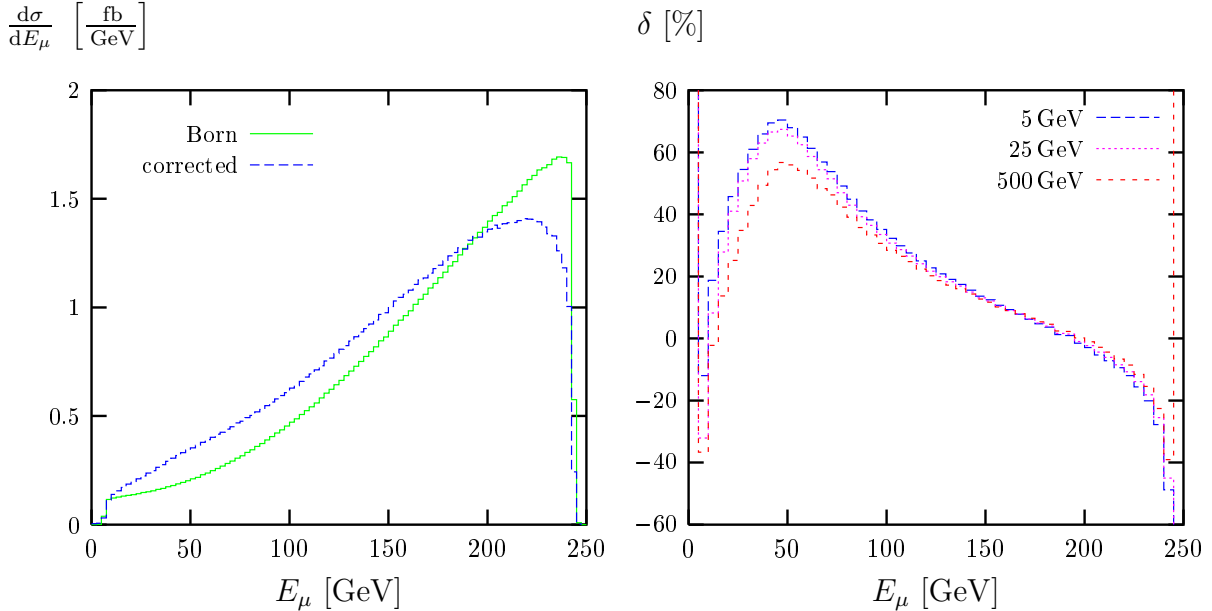


Figure 3: Muon-energy distribution for  $e^+e^- \rightarrow \nu_\mu\mu^+d\bar{u}$  and  $\sqrt{s} = 500$  GeV

Finally, in Figures 4 and 5 we show the distributions of events in the invariant masses of the final-state lepton pair,  $M_{\mu\nu_\mu}$ , and of the final-state quark pair,  $M_{d\bar{u}}$ . The dependence on the recombination cut is sizeable everywhere. The results for the invariant-mass distributions can be understood as follows. For small recombination cuts, in most of the events the  $W$  bosons are defined from the decay fermions only. If a photon is emitted from the decay fermions and not recombined, the invariant mass of the fermions is smaller than the one of the decaying  $W$  boson. This leads to an enhancement of the distribution for invariant masses below the  $W$  resonance. This effect becomes smaller with increasing recombination mass. The enhancement is proportional to the squared charges of the final-state fermion, i.e. it is largest for the leptonic invariant mass. On the other hand, if the recombination mass gets large, the probability increases that the recombined fermion momenta receive contributions from photons that are radiated during the  $W$ -production subprocess or from the decay fermions of the other  $W$  boson. This leads to positive corrections above the considered  $W$  resonance. The effect is larger for the hadronic invariant mass since in this case, two decay fermions (the two quarks) can be combined with the photon. The effect of the squared charges of the final-state fermions is marginal in this case because the contribution of initial-state fermions dominates.

In contrast to LEP2 energies [10] there is a significant difference between the loose recombination cut  $M_{\text{rec}} = 25$  GeV and the full recombination  $M_{\text{rec}} = 500$  GeV. As already explained in Ref. [10], the recombination of a photon that forms an invariant mass of at least 25 GeV with charged fermions shifts the events by at least 3.8 GeV for the leptonically-decaying  $W$  boson and 7.4 GeV for the hadronically-decaying  $W$  boson. Such a shift leads to an increase of the corrections only outside the range shown in Figures 4 and 5. However, in contrast to the LEP2 energy, the phase space for hard photons is very large at  $\sqrt{s} = 500$  GeV, leading to a global significant decrease of the  $W$  line shape near the resonance if the recombination cut  $M_{\text{rec}}$  increases from 25 GeV to 500 GeV.

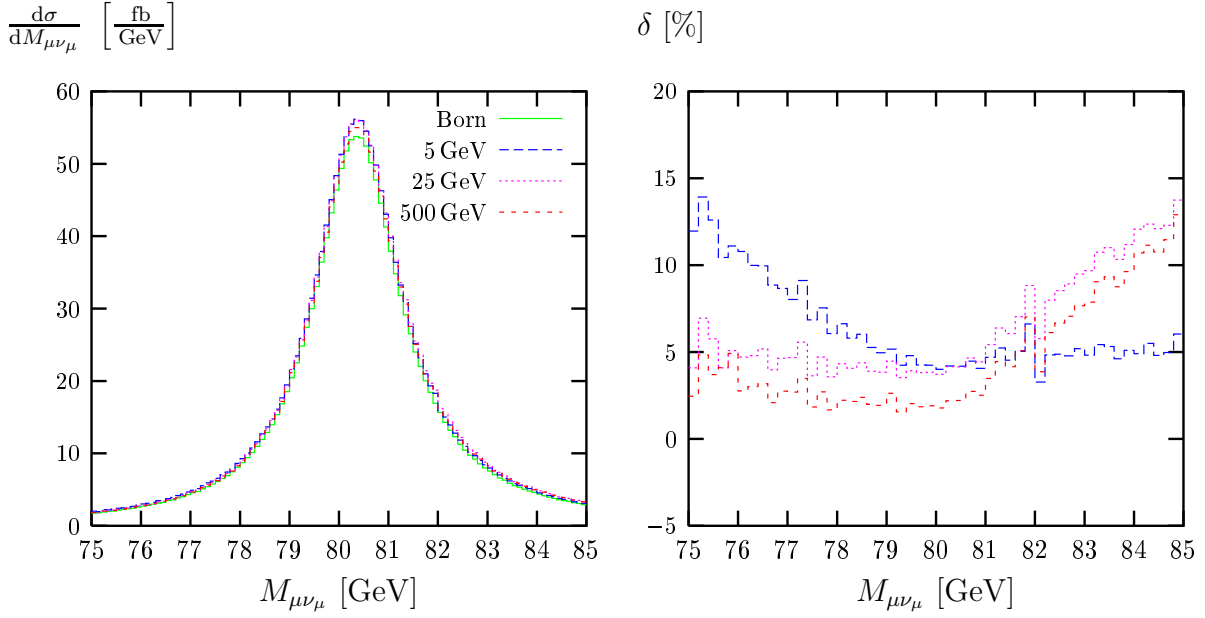


Figure 4: Invariant-mass distribution of the lepton pair for  $e^+e^- \rightarrow \nu_\mu\mu^+d\bar{u}$  and  $\sqrt{s} = 500 \text{ GeV}$

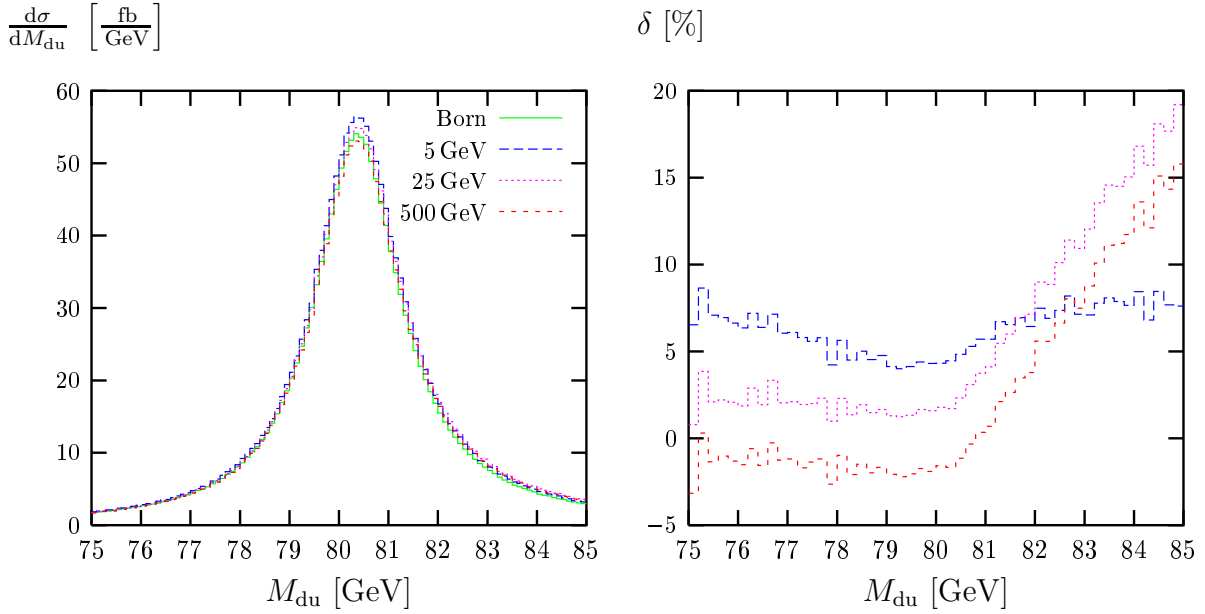


Figure 5: Invariant-mass distribution of the quark pair for  $e^+e^- \rightarrow \nu_\mu\mu^+d\bar{u}$  and  $\sqrt{s} = 500 \text{ GeV}$



	$M_{\text{rec}}$ [GeV]	$M_{W,\text{fit}}^{\text{Born,CC03}}$ [GeV]	$M_{W,\text{fit}}^{\text{Born}}$ [GeV]	$M_{W,\text{fit}}^{\text{corr}}$ [GeV]	$\Delta M_{W,\text{fit}}^{\text{corr}}$ [MeV]
$W^+ \rightarrow \nu_\mu \mu^+$	5	80.377	80.376	80.377	+1
		80.388	80.386	80.386	+0
	25	80.377	80.376	80.389	+13
		80.388	80.386	80.405	+19
	500	80.377	80.376	80.389	+13
		80.388	80.386	80.405	+19
$W^- \rightarrow d\bar{u}$	5	80.378	80.377	80.389	+11
		80.388	80.388	80.402	+14
	25	80.378	80.377	80.401	+23
		80.388	80.388	80.422	+35
	500	80.378	80.377	80.401	+24
		80.388	80.388	80.424	+36

Table 2: Results for  $M_{W,\text{fit}}$  for a Breit–Wigner fit to the invariant-mass distributions shown in Figures 4 and 5, using the fit ranges  $78.3 \text{ GeV} < M < 82.3 \text{ GeV}$  (upper values) and  $76.3 \text{ GeV} < M < 84.3 \text{ GeV}$  (lower values)

The distortion of the W invariant-mass distributions is of particular interest for the reconstruction of the W-boson mass  $M_W$  from the decay products. In order to illustrate the impact of the corrections on the determination of  $M_W$ , we fit the simple Breit–Wigner distribution

$$\left(\frac{d\sigma}{dM^2}\right) = \frac{\text{const.}}{(M^2 - M_{W,\text{fit}}^2)^2 + M_{W,\text{fit}}^2 \Gamma_{W,\text{fit}}^2} \quad (3)$$

to the W line shapes shown in Figures 4 and 5, treating  $M_{W,\text{fit}}$  and  $\Gamma_{W,\text{fit}}$  (as well as the normalization constant) as free fit parameters. We determine the fitted W-boson masses from the predictions resulting from the lowest-order CC03 diagrams,  $M_{W,\text{fit}}^{\text{Born,CC03}}$ , from the complete lowest-order diagrams,  $M_{W,\text{fit}}^{\text{Born}}$ , and from the fully corrected predictions,  $M_{W,\text{fit}}^{\text{corr}}$ . In addition we give the mass shift resulting from the corrections  $\Delta M_{W,\text{fit}}^{\text{corr}} = M_{W,\text{fit}}^{\text{corr}} - M_{W,\text{fit}}^{\text{Born}}$ . The results of these fits, which are contained in Table 2, show that the fitted W-boson mass changes at the order of some 10 MeV if the corrections are included. The mass shift crucially depends on the recombination procedure. From the discussion of the line-shape distortion above it is clear that this mass shift is more positive if more photons are recombined. Moreover, the differences in  $M_{W,\text{fit}}^{\text{corr}}$  between the recombination cuts  $M_{\text{rec}} = 25 \text{ GeV}$  and  $500 \text{ GeV}$  are only marginal, since the corresponding line-shape distortions are practically the same. The results also illustrate that the fit results vary at the order of some 10 MeV for different fit ranges in  $M$ .

In summary, we have applied the event generator RACOONWW for  $e^+e^- \rightarrow WW \rightarrow 4f(+\gamma)$ , which includes the complete  $\mathcal{O}(\alpha)$  electroweak corrections in double-pole approximation, for the linear-collider centre-of-mass energy 500 GeV. With this generator we

have calculated the total cross sections and various distributions of experimental relevance. For angular and energy distributions we find corrections up to several 10%, i.e. they are much larger than at LEP2. Since the bulk of these corrections is due to a redistribution of events by kinematical effects induced by hard-photon radiation, corrections of even higher order are expected to be less drastic. For invariant-mass distributions of the W bosons, the size of the corrections is similar as at LEP2. The detailed numerical discussion demonstrates that the issue of photon recombination is of great importance in view of the aimed accuracy of 15 MeV in the kinematical reconstruction of  $M_W$  at TESLA [ 20].

## References

- [1] M. Böhm et al., *Nucl. Phys.* **B304** (1988) 463.
- [2] J. Fleischer, F. Jegerlehner and M. Zralek, *Z. Phys.* **C42** (1989) 409.
- [3] A. Denner and T. Sack, *Z. Phys.* **C46** (1990) 653.
- [4] D.Yu. Bardin, S. Riemann and T. Riemann, *Z. Phys.* **C32** (1986) 121;  
F. Jegerlehner, *Z. Phys.* **C32** (1986) 425.
- [5] A. Aeppli, G.J. van Oldenborgh and D. Wyler, *Nucl. Phys.* **B428** (1994) 126.
- [6] W. Beenakker, F.A. Berends and A.P. Chapovsky, *Nucl. Phys.* **B548** (1999) 3.
- [7] S. Jadach et al., *Phys. Lett.* **B417** (1998) 326.
- [8] S. Jadach et al., hep-ph/9907436.
- [9] Y. Kurihara, M. Kuroda and D. Schildknecht, hep-ph/9908486.
- [10] A. Denner, S. Dittmaier, M. Roth and D. Wackerroth, hep-ph/9912261.
- [11] W. Beenakker et al., *Phys. Lett.* **B317** (1993) 622 and *Nucl. Phys.* **B410** (1993) 245;  
M. Kuroda and D. Schildknecht, *Nucl. Phys.* **B531** (1998) 24.
- [12] A. Denner, S. Dittmaier, M. Roth and D. Wackerroth, in preparation.
- [13] K. Melnikov and O.I. Yakovlev, *Nucl. Phys.* **B471** (1996) 90;  
W. Beenakker, A.P. Chapovsky and F.A. Berends, *Phys. Lett.* **B411** (1997) 203 and  
*Nucl. Phys.* **B508** (1997) 17.
- [14] A. Denner, S. Dittmaier and M. Roth, *Nucl. Phys.* **B519** (1998) 39 and *Phys. Lett.*  
**B429** (1998) 145.
- [15] V.S. Fadin, V.A. Khoze and A.D. Martin, *Phys. Lett.* **B311** (1993) 311;  
D. Bardin, W. Beenakker and A. Denner, *Phys. Lett.* **B317** (1993) 213;  
V.S. Fadin et al., *Phys. Rev.* **D52** (1995) 1377.
- [16] A. Denner, S. Dittmaier, M. Roth and D. Wackerroth, *Nucl. Phys.* **B560** (1999) 33.

- [17] S. Dittmaier, BI-TP 99/09, hep-ph/9904440, to appear in *Nucl. Phys. B*;  
M. Roth, dissertation ETH Zürich No. 13363, 1999.
- [18] W. Beenakker et al., *Nucl. Phys. B* **500** (1997) 255.
- [19] G. Passarino, hep-ph/9810416;  
E.E. Boos and M.N. Dubinin, hep-ph/9909214;  
A. Ballestrero, hep-ph/9911235.
- [20] E. Accomando et al., *Phys. Rep.* **299** (1998) 1.